Phycoerythrin-specific bilin lyase–isomerase controls blue-green chromatic acclimation in marine *Synechococcus*

Animesh Shukla[a], Avijit Biswas[b], Nicolas Blot[c,d,e], Frédéric Partensky[c,d], Jonathan A. Karty[f], Loubna A. Hammad[f], Laurence Garczarek[c,d], Andrian Gutu[a,g], Wendy M. Schluchter[b], and David M. Kehoe[a,h,1]

[a]Department of Biology, Indiana University, Bloomington, IN 47405; [b]Department of Biological Sciences, University of New Orleans, New Orleans, LA 70148; [c]UPMC-Université Paris 06, Station Biologique, 29680 Roscoff, France; [d]Centre National de la Recherche Scientifique, Unité Mixte de Recherche 7144 Adaptation et Diversité en Milieu Marin, Groupe Plancton Océanique, 29680 Roscoff, France; [e]Clermont Université, Université Blaise Pascal, Unité Mixte de Recherche Centre National de la Recherche Scientifique 6023, Laboratoire Microorganismes: Génome et Environnement, 63000 Clermont-Ferrand, France; [f]METACyt Biochemical Analysis Center, Department of Chemistry, Indiana University, Bloomington, IN 47405; [g]Department of Molecular and Cellular Biology, Harvard University, Cambridge, MA 02138; and [h]Indiana Molecular Biology Institute, Indiana University, Bloomington, IN 47405

Edited by Alexander Namiot Glazer, University of California, Berkeley, CA, and approved October 4, 2012 (received for review July 10, 2012)

The marine cyanobacterium *Synechococcus* is the second most abundant phytoplanktonic organism in the world's oceans. The ubiquity of this genus is in large part due to its use of a diverse set of photosynthetic light-harvesting pigments called phycobiliproteins, which allow it to efficiently exploit a wide range of light colors. Here we uncover a pivotal molecular mechanism underpinning a widespread response among marine *Synechococcus* cells known as "type IV chromatic acclimation" (CA4). During this process, the pigmentation of the two main phycobiliproteins of this organism, phycoerythrins I and II, is reversibly modified to match changes in the ambient light color so as to maximize photon capture for photosynthesis. CA4 involves the replacement of three molecules of the green light-absorbing chromophore phycoerythrobilin with an equivalent number of the blue light-absorbing chromophore phycourobilin when cells are shifted from green to blue light, and the reverse after a shift from blue to green light. We have identified and characterized MpeZ, an enzyme critical for CA4 in marine *Synechococcus*. MpeZ attaches phycoerythrobilin to cysteine-83 of the α-subunit of phycoerythrin II and isomerizes it to phycourobilin. *mpeZ* RNA is six times more abundant in blue light, suggesting that its proper regulation is critical for CA4. Furthermore, *mpeZ* mutants fail to normally acclimate in blue light. These findings provide insights into the molecular mechanisms controlling an ecologically important photosynthetic process and identify a unique class of phycoerythrin lyase/isomerases, which will further expand the already widespread use of phycoerythrin in biotechnology and cell biology applications.

light regulation | marine cyanobacteria | phycobilisomes | fluorescence | liquid chromatography-mass spectrometry

Cyanobacteria within the *Synechococcus* spp. are found in marine environments from the equator to the polar circles, and members of this genus contribute significantly to the total phytoplankton biomass and productivity of the oceans (1–3). Their ubiquity is due in part to their wide pigment diversity (4), which arises mainly from differences in the composition of their light-harvesting antennae or phycobilisomes (PBS). PBS consist of a core and six or eight rods radiating from the core that contain the phycobiliprotein phycocyanin (PC) and one or two types of phycoerythrins (PEs), PEI and PEII (5). All phycobiliproteins are α/β heterodimers that are assembled into hexamers by linkers. PEs may bind two different types of chromophores, green light (GL)-absorbing phycoerythrobilin (PEB) and blue light (BL)-absorbing phycourobilin (PUB). These chromophores are ligated to PE by PEB lyases (6, 7) or PEB–lyase–isomerases, which both attach the chromophore and isomerize it to PUB (8). No PE-specific PEB–lyase–isomerase has been described to date. PUB predominates in *Synechococcus* found in nutrient-poor open ocean waters, vast areas where blue light penetrates deeper than any other color (9).

Marine *Synechococcus* are divided into three major pigment types, with type 1 PBS rods containing only PC, type 2 containing PC and PEI, and type 3 containing PC, PEI, and PEII (4). Type 3 can be further split into four subtypes (3 *A–D*) on the basis of the ratio of the PUB and PEB chromophores bound to PEs. For all pigment types and subtypes, the size and number of PBS may vary with irradiance (10), but only pigment subtype 3d is able to vary its pigmentation in response to changes in ambient light color through a process called type IV chromatic acclimation (hereafter called CA4) (4, 11, 12).

Other CA types, such as CA2 and CA3, have been studied in freshwater cyanobacteria (13, 14). Like CA4, these processes are photoreversible, but they involve very different protein and bilin changes. For example, CA3 in *Fremyella diplosiphon*, which occurs when cells are shifted between red light and GL, involves switching between PC and PE and their corresponding chromophores in the PBS rods (14, 15). In contrast, CA4 occurs when marine *Synechococcus* cells are shifted between GL and BL, and during this process there is no change in the phycobiliprotein composition of the PBS rods (11). Instead, CA4 involves changes in the chromophores associated with two different cysteines within the α-PEII subunit (12). In GL, PEB is bound to these sites, whereas in BL, PUB is bound. The mechanism(s) controlling these changes is unknown. Here, we use biochemical and molecular genetic approaches to describe MpeZ, an enzyme involved in the ligation and isomerization of a PEII-linked chromophore, and demonstrate its pivotal role in the poorly understood but globally important process of CA4. The discovery of this class of enzymes has the potential to further expand the current broad use of phycoerythrin in biotechnology and cell biology applications.

Results

Comparative genomics analysis showed that all sequenced marine *Synechococcus* strains that undergo CA4 possess a specific gene, called *mpeZ* (4). In *Synechococcus* sp. RS9916 (hereafter 9916), *mpeZ* is downstream of a gene of unknown function and overlaps a gene putatively encoding a truncated form of the photosystem II core protein PsbA (Fig. 1*A*). RNA blot analysis demonstrated that *mpeZ* transcript accumulation was CA4 regulated, being six times more abundant in cells grown in BL than in GL (Fig. 1*B*). Primary

Author contributions: A.S., A.B., N.B., F.P., J.A.K., L.A.H., L.G., A.G., W.M.S., and D.M.K. designed research; A.S., A.B., N.B., J.A.K., L.A.H., A.G., W.M.S., and D.M.K. performed research; A.S., N.B., J.A.K., L.A.H., and D.M.K. contributed new reagents/analytic tools; A.S., A.B., N.B., F.P., J.A.K., L.A.H., L.G., W.M.S., and D.M.K. analyzed data; and A.S., A.B., F.P., J.A.K., L.A.H., L.G., W.M.S., and D.M.K. wrote the paper.

The authors declare no conflict of interest.

This article is a PNAS Direct Submission.

[1]To whom correspondence should be addressed. E-mail: dkehoe@indiana.edu.

This article contains supporting information online at www.pnas.org/lookup/suppl/doi:10.1073/pnas.1211777109/-/DCSupplemental.

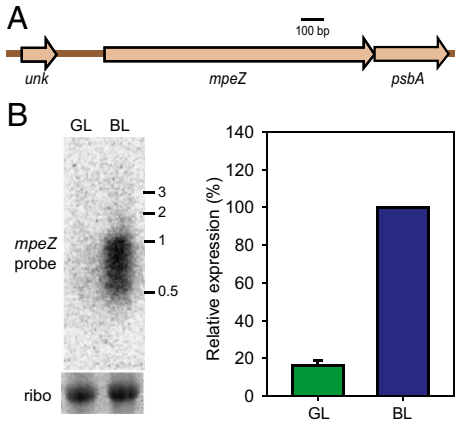

Fig. 1. *mpeZ* genome localization and expression. (*A*) *mpeZ* genome context: "*psbA*" denotes a fragment of *psbA*; "*unk*" denotes an unknown gene. (*B*) (*Left*) Representative RNA blot of transcripts from cells acclimated to GL or BL using *mpeZ* and 16S rRNA (ribo) probes. Numbers are lengths in kbp. (*Right*) Relative mean transcript levels of *mpeZ* in 9916 cells grown in GL or BL. Values expressed as a percentage of transcripts from BL-grown cells after ribo normalization. Data are from three independent RNA blot analyses; error bars show SE.

and secondary structure analyses of the encoded protein, MpeZ, revealed a large domain belonging to the PBS lyase HEAT-like repeat family (Fig. S1*A*), suggesting that this protein could be a bilin lyase–isomerase involved in mediating the shift between PEB- and PUB-enriched PBS rods during CA4.

MpeZ was tested for lyase–isomerase activity by producing it in *Escherichia coli* cells expressing *ho1* and *pebS*, which encode the proteins needed for the synthesis of PEB (16), along with six-histidine–tagged (HT) versions of wild-type (WT) and mutant forms of either MpeA (PEII α-subunit) or CpeA (PEI α-subunit). Spectral analyses of purified wild-type HT-MpeA from MpeZ-containing *E. coli* cells revealed absorbance and fluorescence emission maxima at 495 and 510 nm, respectively (Fig. 2*A*), which matched the spectral properties of PUB attached to protein (8, 18, 19). HT-MpeA was detectable on protein gels and contained an attached bilin (Fig. 2*C*). As expected, no absorbance or fluorescence was detectable from HT-MpeA expressed in cells lacking MpeZ (Fig. 2 *A* and *C*) because nonchromophorylated recombinant PE subunits are generally insoluble in *E. coli* (6, 20). There are three canonical chromophore-binding cysteines at positions 75, 83, and 140 within MpeA. These cysteines were mutated to alanine in various combinations and expressed in *E. coli* cells producing MpeZ and PEB. The spectral properties of purified HT-MpeA-C75A,C140A matched those of HT-MpeA, whereas HT-MpeA-C83A showed no absorbance or fluorescence, indicating that the latter form was nonchromophorylated (Fig. 2 *B* and *C*) (6, 20). When MpeZ was coexpressed with HT-CpeA in the PEB-producing *E. coli* strain, the HT-CpeA protein showed no absorbance or fluorescence, indicating that, in this *E. coli* system, MpeZ does not chromophorylate CpeA (Fig. 2*B*). From these data we conclude that, when expressed in *E. coli*, MpeZ functions as a phycobilin lyase–isomerase, attaching PEB at Cys-83 of MpeA and isomerizing it to PUB (Fig. 2*D*).

To further analyze the role of MpeZ, we created an *mpeZ* insertion mutant in 9916 (Fig. S2) and tested it for its ability to carry out CA4 by recording the $Ex_{495\ nm}$:$Ex_{550\ nm}$ fluorescence excitation ratio, with emission set at 580 nm (hereafter $Ex_{495:550}$), which has been used previously as a proxy for assessing the in vivo PUB:PEB ratio (12). For "control" cultures (cells with normal CA4, carrying the same antibiotic resistance marker as the *mpeZ* insertion mutant) acclimated to GL and then switched to BL, the $Ex_{495:550}$ increased from 0.7 to 1.5 over a 6-d period and subsequently remained constant (Fig. 3*A*). In contrast, this ratio steadily rose from 0.7 to 0.9 for *mpeZ* mutant cultures over the 11-d experi-

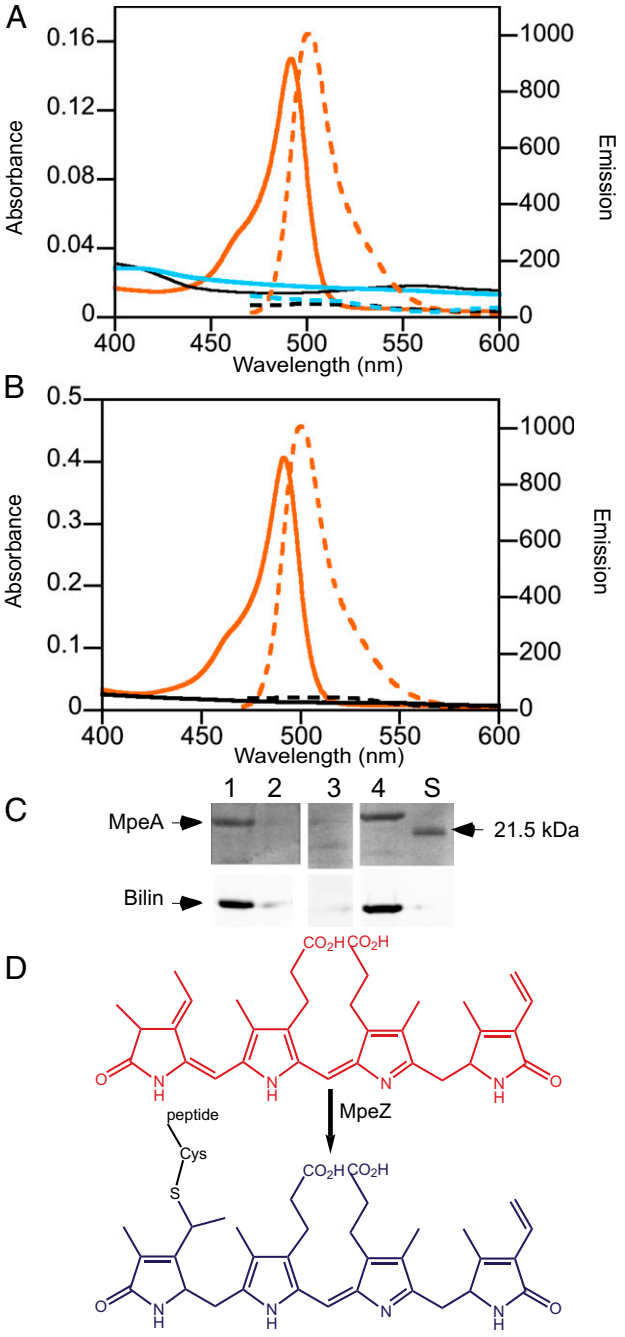

Fig. 2. Analyses of recombinant HT-MpeA and HT-CpeA produced in presence or absence of MpeZ. (*A*) Absorbance (solid lines) and fluorescence emission (dashed lines) spectra for (*i*) HT-MpeA purified from cells containing MpeA, PEB (17), and MpeZ (orange); (*ii*) HT-MpeA purified from cells containing MpeA and PEB only (no MpeZ; black); and (*iii*) HT-CpeA purified from cells containing CpeA and PEB and MpeZ (aqua). (*B*) Absorbance (solid lines) and fluorescence emission (dashed lines) spectra for MpeA with cysteinyl-binding sites replaced by alanines as (*i*) HT-MpeA-C75A,C140A purified from cells containing MpeA-C75A,C140A and PEB and MpeZ (orange) and (*ii*) HT-MpeA-C83 purified from cells containing MpeA-C83A, PEB, and MpeZ (black). (*C*) (*Upper*) Coomassie-stained SDS polyacrylamide gel with HT-MpeA purified from cells containing MpeA, PEB with (lane 1) or without (lane 2) MpeZ, from cells with MpeA-C83A, PEB, and MpeZ (lane 3) or from cells containing MpeA-C75A, C140A, PEB, and MpeZ (lane 4). The molecular mass of the standard loaded in lane "S" is indicated on the right. (*Lower*) Zinc-enhanced fluorescence of bilins within the above gel. (*D*) The chemical reaction catalyzed by MpeZ is the attachment of PEB (red) to a cysteine residue of a MpeA apoprotein (black) and its isomerization to PUB (blue).

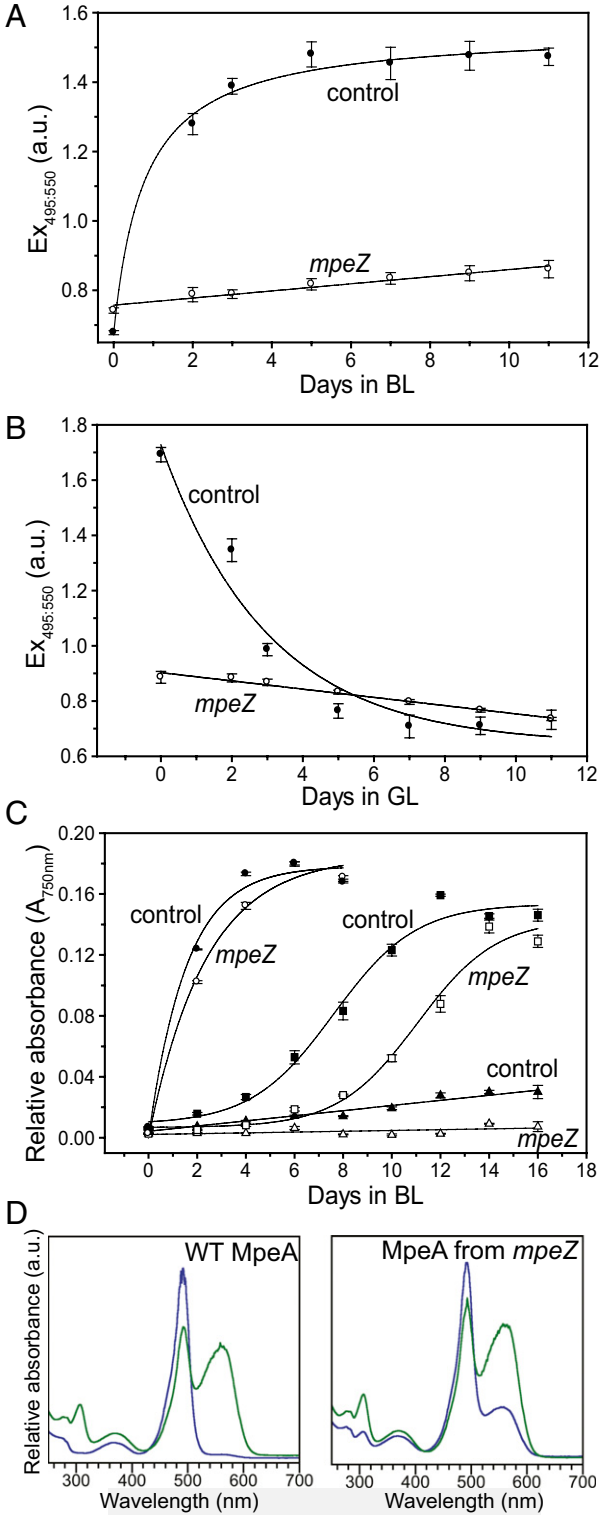

Fig. 3. Effect of *mpeZ* disruption on spectral properties and growth of 9916 cells. (*A*) $Ex_{495:550}$ from control (closed circles) and *mpeZ* mutant (open circles) cells grown in GL and then shifted to BL at time 0. (*B*) $Ex_{495:550}$ from the same cell cultures grown in BL and then shifted to GL at time 0. (*C*) Growth curves for control (closed symbols) and *mpeZ* mutant (open symbols) cells grown at different BL irradiances: circles, squares, and triangles correspond to 15, 5, and 1 μmol photons $m^{-2}{\cdot}s^{-1}$, respectively. (*D*) Absorption spectra of the MpeA protein purified from WT (*Left*) or *mpeZ* mutant cells (*Right*) grown in BL (blue line) and GL (green line).

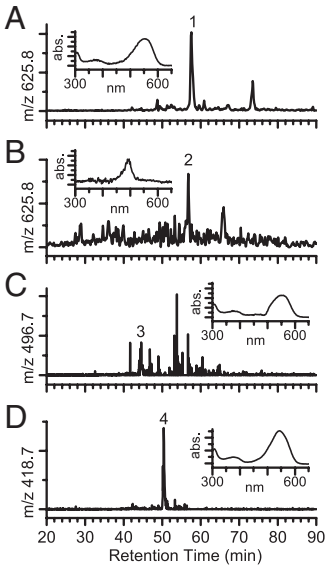

Fig. 4. EICs and UV-VIS absorption spectra for tryptic peptides containing C83 of MpeA isolated from WT 9916 and *mpeZ* mutant cells grown in BL or GL. (*A*) EIC for the peptide $EKC_{83}KR\ (M+2H)^{2+}$ at *m/z* 625.8 derived from WT cells grown in GL. (*Inset*) UV-VIS absorption spectrum for the peak at retention time 57.5 min ("1" on the chromatogram) indicates PEB on C83. abs., absorbance. (*B*) EIC for the peptide $EKC_{83}KR\ (M+2H)^{2+}$ at *m/z* 625.8 derived from BL-grown WT cells. (*Inset*) UV-VIS absorption spectrum for the peak at 57.4 min ("2" on the chromatogram) indicates PUB on C83. (*C*) EIC for the peptide $C_{83}KR\ (M+2H)^{2+}$ at *m/z* 496.7 derived from GL-grown *mpeZ* mutant cells. (*Inset*) UV-VIS absorption spectrum for the peak at retention time 44.6 min ("3" on the chromatogram) indicates PEB on C83. (*D*) EIC for the peptide $C_{83}K\ (M+2H)^{2+}$ at *m/z* 418.7 derived from BL-grown *mpeZ* mutant cells. (*Inset*) UV-VIS absorption spectrum at 50.0 min ("4" on the chromatogram) indicates PEB on C83.

mental period. Complementary responses were obtained for control and *mpeZ* mutant cultures when BL-acclimated cells were shifted to GL (Fig. 3*B*). Thus, compared with the control, the loss of MpeZ activity resulted in a 75% decrease in the difference between the $Ex_{495:550}$ value in BL versus GL, and this was attributable to the lower $Ex_{495:550}$ value in BL. Control and *mpeZ* mutant cell growth was measured at three BL irradiances (Fig. 3*C*). Growth was similar for the two cultures at 15 μmol photons $m^{-2}{\cdot}s^{-1}$ but was much slower in the mutant at 5 μmol photons $m^{-2}{\cdot}s^{-1}$. At 1 μmol photons $m^{-2}{\cdot}s^{-1}$, the control cells grew slowly whereas *mpeZ* mutant cells showed virtually no growth. Thus, in BL, the disruption of *mpeZ* affected both the fluorescence characteristics of the PBS and growth, especially at low irradiances.

To identify the rod proteins that are acted upon by MpeZ in vivo, the PEI and PEII α and β subunits (CpeA, CpeB, MpeA and MpeB) were isolated from 9916 wild type and *mpeZ* mutant cells grown in BL and GL (Fig. S3 *A* and *B*). The identity of proteins in each of the major peaks was confirmed by mass spectrometry (MS). No difference was observed between the HPLC profiles of phycobiliproteins from wild-type and *mpeZ* mutant cells. Comparison of the 280 nm absorbance chromatograms (Fig. S3 *A* and *B*), did not reveal significant differences in the CpeA:MpeA and CpeB:MpeB ratios in WT and *mpeZ* mutant cells in either light condition. Spectral analysis of isolated MpeA demonstrated that the absorption spectra were the same for wild-type and the *mpeZ* mutant in GL but differed in BL, where PEB absorbance was detectable in the mutant but not in wild-type cells (Fig. 3*D*). Similar analyses of isolated CpeA showed that the PUB:PEB absorbance ratios were the same in the wild-type and *mpeZ* mutant cultures in BL and GL (Fig. S3 *C* and *D*). These data demonstrate that MpeZ is involved in the attachment of PUB to MpeA, but not CpeA, in BL-grown wild-type 9916 cells.

The type of bilins attached to the major PBS rod proteins of wild-type and *mpeZ* mutant cells grown in BL and GL was determined using parallel UV-visible (UV-VIS) spectroscopy and tandem MS of HPLC-purified proteins. The MS peak intensities (extracted ion chromatograms, or EICs) and UV-VIS spectra for MpeA-C83 tryptic peptides are provided in Fig. 4, and those for MpeA-C75 and MpeA-C140 tryptic peptides are provided in Fig. S4. Similar data for peptides containing CpeA-C82 and CpeA-C139 are presented in Figs. S5 and S6. The results for the HPLC purification and spectral analysis of CpeB and MpeB from wild type and the *mpeZ* mutant are shown in Fig. S7; the UV-VIS spectra and MS peak intensities for tryptic peptides containing the four chromophore-binding cysteines of CpeB, the two chromophore-binding cysteines of MpeB, and the single chromophore-binding cysteine of RpcA, encoding the PC α subunit, are provided in Fig. S8. The data extracted from all of these analyses is summarized in Table 1 and show that CpeA-C139, MpeA-C83, and MpeA-C140 are the three amino acids that undergo changes in bilin composition during CA4. In wild-type cells, each has PEB attached in GL and PUB attached in BL, whereas in the *mpeZ* mutant MpeA-C83 fails to attach PUB in BL. These data confirm that the role of MpeZ in CA4 is to ligate PUB to MpeA-C83 during growth in BL.

Discussion

CA4 is a sophisticated physiological mechanism by which some marine *Synechococcus* strains can finely tune the absorption properties of their antenna complexes to the ambient light color (4, 11). Here we show that MpeZ, present in all *Synechococcus* strains sequenced to date that carry out CA4, is a key enzyme in this process. This enzyme is unique among phycobilin lyase–isomerases described so far because it chromophorylates phycoerythrin, specifically PEII (MpeA). The only other such enzymes known are PecE/PecF, which bind phycocyanobilin at C84 of the phycoerythrocyanin α-subunit and isomerize it to a phycoviolobilin (21, 22), and RpcG, which ligates PEB at C84 of a phycocyanin α-subunit and isomerizes it to PUB (8). All three enzymes belong to the E/F clan of phycobilin lyases, characterized by the presence of an α/α-superhelix fold and Armadillo repeat motifs (23–25), although MpeZ is only distantly related to PecE (27–32% identity and 45–47% homology) and the N terminus of RpcG (23–25% identity and 42–43% homology) and matches just a short part of PecF (29% identity and 53–55% homology over 57 residues) (Fig. S1*B*). It is particularly interesting that the conserved motif of PecF and the PecF-like C terminus of RpcG that is involved in isomerization, NHCQGN (underlined in Fig. S1*B*), is absent in MpeZ (8, 26).

Our results are consistent with MpeZ's role in the isomerization of PEB to PUB and its attachment at MpeA-C83 in BL. MS analyses revealed that the *mpeZ* mutant possesses a PEB at MpeA-C83 in both BL and GL, indicating that PEB lyase activity is retained at this position. Although unlikely, we cannot rule out the possibility that the *mpeZ* mutant is producing a form of MpeZ that has kept its PEB ligation activity but lost its isomerase activity. It is also possible that another lyase is adding PEB to MpeA-83 in BL when MpeZ is absent. Recently, it was demonstrated that CpeY was involved in binding a PEB to CpeA-C82 from *Fremyella diplosiphon* (6) and that this reaction was facilitated by the presence of CpeZ. Because orthologs of CpeY/CpeZ are present in 9916, they very likely catalyze binding of PEB to CpeA-C82. We

Table 1. Chromophores found at different cysteinyl sites for phycobiliproteins examined in WT and *mpeZ* cultures grown in BL and GL

Protein	PUB:PEB ratio in GL	PUB:PEB ratio in BL	Cysteine position	Bilin in GL	Bilin in BL
CpeA-WT	2PEB	**1PUB:1PEB**	82	PEB*	PEB*
			139	**PEB***	**PUB***
MpeA-WT	1PUB:2PEB	**3PUB**	75	PUB*	PUB*
			83	**PEB***	**PUB***
			140	**PEB***	**PUB***
CpeB-WT	1PUB:2PEB	1PUB:2PEB	50, 61	PUB*	PUB*
			82	PEB	PEB*
			165	PEB*	PEB*
MpeB-WT	1PUB:2PEB	1PUB:2PEB	50, 61	PUB	PUB
			82	PEB	PEB
			159	PEB*	PEB
RpcA-WT			84	PUB	PUB
RpcB-WT			82	PCB	PCB
			153	PEB	PEB
MpeC-WT	1PUB	1PUB	49	PUB	PUB
CpeA-*mpeZ*	2PEB	**1PUB:1PEB**	82	PEB*	PEB*
			139	**PEB***	**PUB***
MpeA-*mpeZ*	1PUB:2PEB	**2PUB:1PEB**	75	PUB*	PUB*
			83	PEB*	PEB*
			140	**PEB***	**PUB***
CpeB-*mpeZ*	1PUB:2PEB	1PUB:2PEB	50, 61	PUB*	PUB*
			82	PEB*	PEB*
			165	PEB*	PEB*
MpeB-*mpeZ*	1PUB:2PEB	1PUB:2PEB	50, 61	PUB*	PUB*
			82	PEB*	PEB*
			159	PEB*	PEB*
RpcA-*mpeZ*			84	PUB*	PUB
RpcB-*mpeZ*			82	PCB	PCB
			153	PEB	PEB
MpeC-*mpeZ*	1PUB	1PUB	49	PUB	PUB

The differences between BL and GL resulting from CA4 are highlighted in boldface type, and the only difference between WT and mutant cells is underlined.
*These bilins were confirmed by LC/MS/MS (Fig. 4 and Figs. S4, S5, and S8).

hypothesize that CpeY (+CpeZ) may also add PEB to MpeA-C83 in GL while MpeZ adds PUB in BL, and these may be the lyases/lyase–isomerases that collectively control the CA4-regulated change of chromophorylation at C83 on MpeA.

CA4-mediated changes in chromophorylation at the other two sites, CpeA-C139 and MpeA-C140 (Table 1), are likely mediated by one or two additional lyase/lyase–isomerase pair(s) that have not been identified yet. Alternatively, a separate PUB synthesis pathway could exist that, in concert with the PEB synthesis pathway, increases the PUB:PEB ratio in BL and decreases it in GL. Also, although we cannot exclude the possibility that chromophore attachment occurs autocatalytically, we believe that this hypothesis is less likely because such in vivo chromophore attachment has not been reported for phycobiliproteins.

An unexpected result from this study is that, although MpeZ appears to be responsible for the chromophorylation of only one of the three sites that change chromophores during CA4, there was a 75% decrease in the difference between the $Ex_{495:550}$ value in BL versus in GL (Fig. 3 *A* and *B*). This is a more dramatic decrease than might have been expected for a single chromophore change, but may be due in part to the position of the MpeA-C83 chromophore in the energy transfer flow within a PE hexamer. The structure of R-PE of *Polysiphonia urceolata* allowed distance measurements between bilins within a PE hexamer and estimates of likely energy transfer pathways (27). PEB at CpeA-C83 played a critical role in transferring energy from the chromophores located on the outside of the PE hexamer (i.e., β50/61-PUB and α140-PEB in *P. urceolata*) to the terminal PEB acceptor located at β82 (5, 27). In 9916 cells grown in BL, the two external chromophores are β50/61-PUB and α140-PUB. In the *mpeZ* mutant, PEB at MpeA-C83 instead of the PUB in wild-type cells (Table 1) may alter relaxation constraints within PEII and/or result in different spectral overlaps with the other bilins present within the hexamer, allowing for dissipation of the excited state by mechanisms other than fluorescence. Quantum yield and fluorescence lifetime measurements for PEII from BL-grown 9916 wild-type and *mpeZ* mutant cells should resolve this issue.

By allowing marine *Synechococcus* strains to alter their pigment ratios to match the ambient light color environment, CA4 is likely to confer a fitness advantage over those strains that have fixed pigmentation in habitats where the ratio of blue to green light varies frequently (4). Such an advantage appears to be conferred by CA3, which is beneficial in environments where the red- to green-light ratio varies over time periods longer than the CA3 acclimation time (28). Given the remarkable ubiquity and abundance of marine *Synechococcus* in the world's oceans, CA4 must be a globally significant light color acclimation process. The discovery of the first lyase–isomerase controlling CA4 confirms previous proposals that such an enzyme(s) is critical for this response (4, 12). Two other forms of chromatic acclimation that have been analyzed, CA2 and CA3, are complex responses that involve changes in the expression of genes encoding phycobiliprotein and bilin biosynthetic enzymes (14). The fact that MpeZ is a PEII PEB lyase–isomerase, together with data showing that the composition of phycobiliproteins in the rods does not change during CA4 (12), demonstrates that CA4 is fundamentally different from other forms of CA and is likely to be regulated through different light sensing and signal transduction mechanisms (14).

The discovery of MpeZ provides a valuable addition to the array of phycobilin lyases available for producing natural or artificial phycobiliproteins for medical and biological research and industry (29, 30). Because PEB-containing PE conjugated to antibodies or other proteins is currently widely used in bioimaging and cell-sorting applications due to its superior fluorescent properties, MpeZ will be a valuable tool for producing PUB-containing PE for in vivo biotechnological applications.

Materials and Methods

Strains and Growth Conditions. RS9916, isolated from 10 m deep in the Gulf of Aqaba (31), was obtained from the Roscoff Culture Collection (strain no. RCC555) (4). Wild-type or *mpeZ* mutant *Synechococcus* RS9916 cells were grown at 22 °C in PCR-S11 (32) with or without 50 μg/mL kanamycin in polycarbonate Nalgene culture flasks in continuous light using Chroma75 T12 fluorescent bulbs (General Electric). Cultures were acclimated for at least 7 d in BL or GL using filters (LE716 Mikkel Blue, LE738 Jas Green; LEE Filters) at 15 μmol photons $m^{-2}{\cdot}s^{-1}$ unless noted. Photon flux was measured with a Li-Cor LI-250 light meter connected to a LI109SA quantum sensor. Fluorescence excitation spectra were measured using a Biotek Synergy-Mx spectrofluorimeter and used to calculate the $Ex_{495:550}$.

Plasmid Construction. Plasmids used are listed in Table S1 and primers in Table S2. pASmpeZ was made by PCR amplification of an ~800-nucleotide internal region of *mpeZ* using primers mpeZ-internal-for and mpeZ-internal-rev, cutting with BamHI and inserting into similarly cut pMUT100 (33). The cloning junctions and inserted *mpeZ* fragment were sequenced. One expression vector used was previously described (16). RS9916 *mpeA* and RS9916 *cpeA* were amplified using the corresponding primers listed in Table S2. Amplified fragments were cloned in the pCOLA-Duet (Novagen) vector using BamHI-SalI to generate pCOLADuet-RS9916mpeA and into the BamHI and HindIII sites to create pCOLADuet-RS9916cpeA. RS9916 *mpeZ* was PCR-amplified and cloned into BglII/XhoI-cut pCDF-Duet (Novagen) to create pCDF-RS9916mpeZ. The *mpeA* and *cpeA* sequences were inserted into pCOLADuet in frame with the sequence encoding a HT. Single amino acid changes in *mpeA* were made using fusion PCR amplification and the primers listed in Table S2. All cloning junctions and PCR-amplified regions were sequenced.

***mpeZ* Disruption.** pASmpeZ was transformed into *E. coli* MC1061 (34) containing pRK24 (35) and pRL528 (36). Biparental mating of exponentially growing RS9916 and *E. coli* cells was conducted as described (33), except that 9916 cells were grown in BL and then kept in darkness for 2 d before mating for a minimum of 72 h at 30 °C. Cells were plated as previously described (33), except that plates were kept at 22 °C at 5 μmol photons $m^{-2}{\cdot}s^{-1}$ for the first 3 d and then transferred to 15 μmol photons $m^{-2}{\cdot}s^{-1}$. Individual colonies were picked and tested for *mpeZ* disruption using PCR amplification, nucleotide sequencing, and DNA blot analysis using a probe for *mpeZ*.

RNA Analyses. One hundred milliliters of wild-type 9916 cells at a density of ~10^8 cells mL^{-1} and grown in BL or GL were used for RNA analysis as previously described (37), using 10 μg/lane of RNA and a *mpeZ* probe radiolabeled as for the DNA blot.

Recombinant Protein Expression and Purification. Expression plasmids were cotransformed into *E. coli* BL21 (*DE3*) cells and colonies were selected on Luria Bertani (LB) plates with the appropriate antibiotics as described in ref. 6. To produce recombinant proteins, a single colony was inoculated into a 200-mL overnight culture in LB medium with the appropriate antibiotics and shaken at 20 °C at 180 × *g* for 30–48 h until the optical density reached $OD_{600\ nm}$ = 0.6. Production of T7 RNA polymerase was induced by the addition of 0.5 mM isopropyl β-D thiogalactoside. Cells were incubated with shaking at 180 × *g* at 20 °C for another 48 h before harvest by centrifugation. Cell pellets were immediately processed for protein purification as previously described (38). The entire purification process was carried out in the dark at 4 °C. Following dialysis to remove imidazole, spectroscopic measurements were taken immediately.

Protein and Bilin Analysis. Polypeptides were resolved by SDS/PAGE (15%, wt/vol), and polypeptides were visualized by staining with Coomassie Brilliant Blue R-250. Fluorescence from bilins linked to proteins was detected with excitation at 488 nm as described in ref. 6.

Fluorescence Emission and Absorbance Spectra of Purified Proteins. Fluorescence emission and absorbance spectra were recorded as described in ref. 6.

HPLC Separation of Phycobiliproteins. PBS were purified as described (39). HPLC was used to separate each phycobiliprotein as described in the legend for Fig. S3. LC/MS/MS analyses were performed on fractions collected from a C4 column and digested with trypsin as described previously (6).

Analysis of Phycobiliproteins by liquid chromatographic, ultraviolet-visible absorption spectroscopy/tandem mass spectrometry. HPLC-separated and trypsin-digested phycobiliprotein samples from WT or *mpeZ* mutant cells grown in BL or GL were separated by capillary HPLC as described in the legend for Fig. S4. The UV-VIS detector recorded absorption spectra from 250 to 750 nm at 2.5 Hz. Tandem mass spectra were recorded and analyzed as described in the legend for Fig. S4.

ACKNOWLEDGMENTS. We thank David Scanlan, Bianca Brahamsha, and Brian Palenik for providing materials and suggesting methods for growing and transforming 9916. This work was supported by grants to F.P. and L.G. from the Agence Nationale de la Recherche program PELICAN (contract ANR-09-GENM-030) and the European program MicroB3 (Seventh Framework Program contract 287589); an International Projects and Activities Grant from the Office of International Programs at Indiana University (to D.M.K.); and National Science Foundation Grants MCB-1029414 (to D.M.K.) and MCB-0843664 (to W.M.S.). The METACyt Biochemical Analysis Center was supported by a grant from The Lilly Foundation.

1. Olson RJ, Chisholm SW, Zettler ER, Armbrust EV (1990) Pigments, size, and distribution of *Synechococcus* in the North Atlantic and Pacific Oceans. *Limnol Oceanogr* 35(1): 45–58.
2. Partensky F, Blanchot J, Vaulot D (1999) Differential distribution and ecology of *Prochlorococcus* and *Synechococcus* in oceanic waters: A review. *Marine Cyanobacteria*, eds Charpy L, Larkum A (Musée Océanographique, Monaco), Vol 19, pp 457–475.
3. Zwirglmaier K, et al. (2008) Global phylogeography of marine *Synechococcus* and *Prochlorococcus* reveals a distinct partitioning of lineages among oceanic biomes. *Environ Microbiol* 10(1):147–161.
4. Six C, et al. (2007) Diversity and evolution of phycobilisomes in marine *Synechococcus* spp.: A comparative genomics study. *Genome Biol* 8(12):R259.
5. Ong LJ, Glazer AN (1991) Phycoerythrins of marine unicellular cyanobacteria. I. Bilin types and locations and energy transfer pathways in *Synechococcus* spp. phycoerythrins. *J Biol Chem* 266(15):9515–9527.
6. Biswas A, et al. (2011) Characterization of the activities of the CpeY, CpeZ, and CpeS bilin lyases in phycoerythrin biosynthesis in *Fremyella diplosiphon* strain UTEX 481. *J Biol Chem* 286(41):35509–35521.
7. Wiethaus J, et al. (2010) CpeS is a lyase specific for attachment of 3Z-PEB to Cys82 of beta-phycoerythrin from *Prochlorococcus marinus* MED4. *J Biol Chem* 285(48):37561–37569.
8. Blot N, et al. (2009) Phycourobilin in trichromatic phycocyanin from oceanic cyanobacteria is formed post-translationally by a phycoerythrobilin lyase-isomerase. *J Biol Chem* 284(14):9290–9298.
9. Morel A, et al. (2007) Optical properties of the "clearest" natural waters. *Limnol Oceanogr* 52(1):217–229.
10. Six C, Thomas JC, Brahamsha B, Lemoine Y, Partensky F (2004) Photophysiology of the marine cyanobacterium *Synechococcus* sp. WH8102, a new model organism. *Aquat Microb Ecol* 35:17–29.
11. Palenik B (2001) Chromatic adaptation in marine *Synechococcus* strains. *Appl Environ Microbiol* 67(2):991–994.
12. Everroad C, et al. (2006) Biochemical bases of type IV chromatic adaptation in marine *Synechococcus* spp. *J Bacteriol* 188(9):3345–3356.
13. Tandeau de Marsac N (1983) Phycobilisomes and complementary chromatic adaptation in cyanobacteria. *Bull Inst Pasteur* 81:201–254.
14. Gutu A, Kehoe DM (2012) Emerging perspectives on the mechanisms, regulation, and distribution of light color acclimation in cyanobacteria. *Mol Plant* 5(1):1–13.
15. Grossman AR (2003) A molecular understanding of complementary chromatic adaptation. *Photosynth Res* 76(1–3):207–215.
16. Dammeyer T, Bagby SC, Sullivan MB, Chisholm SW, Frankenberg-Dinkel N (2008) Efficient phage-mediated pigment biosynthesis in oceanic cyanobacteria. *Curr Biol* 18(6): 442–448.
17. Dammeyer T, Hofmann E, Frankenberg-Dinkel N (2008) Phycoerythrobilin synthase (PebS) of a marine virus. Crystal structures of the biliverdin complex and the substrate-free form. *J Biol Chem* 283(41):27547–27554.
18. Glazer AN, Hixson CS (1977) Subunit structure and chromophore composition of rhodophytan phycoerythrins. *Porphyridium cruentum* B-phycoerythrin and b-phycoerythrin. *J Biol Chem* 252(1):32–42.
19. Bryant DA, Cohen-Bazire G, Glazer AN (1981) Characterization of the biliproteins of *Gloeobacter violaceus*: Chromophore content of a cyanobacterial phycoerythrin carrying phycourobilin chromophore. *Arch Microbiol* 129(3):190–198.
20. Fairchild CD, Glazer AN (1994) Nonenzymatic bilin addition to the α subunit of an apophycoerythrin. *J Biol Chem* 269(46):28988–28996.
21. Jung LJ, Chan CF, Glazer AN (1995) Candidate genes for the phycoerythrocyanin alpha subunit lyase. Biochemical analysis of *pecE* and *pecF* interposon mutants. *J Biol Chem* 270(21):12877–12884.
22. Storf M, et al. (2001) Chromophore attachment to biliproteins: Specificity of PecE/PecF, a lyase-isomerase for the photoactive 3(1)-cys-alpha 84-phycoviolobilin chromophore of phycoerythrocyanin. *Biochemistry* 40(41):12444–12456.
23. Andrade MA, Petosa C, O'Donoghue SI, Müller CW, Bork P (2001) Comparison of ARM and HEAT protein repeats. *J Mol Biol* 309(1):1–18.
24. Morimoto K, Nishio K, Nakai M (2002) Identification of a novel prokaryotic HEAT-repeats-containing protein which interacts with a cyanobacterial IscA homolog. *FEBS Lett* 519(1–3):123–127.
25. Morimoto K, Sato S, Tabata S, Nakai M (2003) A HEAT-repeats containing protein, IaiH, stabilizes the iron-sulfur cluster bound to the cyanobacterial IscA homologue, IscA2. *J Biochem* 134(2):211–217.
26. Zhao KH, et al. (2005) Amino acid residues associated with enzymatic activities of the isomerizing phycoviolobilin-lyase PecE/F. *Biochemistry* 44(22):8126–8137.
27. Jiang T, Zhang JP, Liang DC (1999) Structure and function of chromophores in R-Phycoerythrin at 1.9 A resolution. *Proteins* 34(2):224–231.
28. Stomp M, et al. (2008) The timescale of phenotypic plasticity and its impact on competition in fluctuating environments. *Am Nat* 172(5):169–185.
29. Sekar S, Chandramohan M (2008) Phycobiliproteins as a commodity: Trends in applied research, patents and commercialization. *J Appl Phycol* 20(2):113–136.
30. Glazer A (1994) Phycobiliproteins: A family of valuable, widely used fluorophores. *J Appl Phycol* 6(2):105–112.
31. Fuller NJ, et al. (2003) Clade-specific 16S ribosomal DNA oligonucleotides reveal the predominance of a single marine *Synechococcus* clade throughout a stratified water column in the Red Sea. *Appl Environ Microbiol* 69(5):2430–2443.
32. Rippka R, et al. (2000) *Prochlorococcus marinus* Chisholm et al. 1992 subsp. *pastoris* subsp. nov. strain PCC 9511, the first axenic chlorophyll a_2/b_2-containing cyanobacterium (Oxyphotobacteria). *Intl J Syst Evol Microbiol* 50(Pt 5):1833–1847.
33. Brahamsha B (1996) A genetic manipulation system for oceanic cyanobacteria of the genus *Synechococcus*. *Appl Environ Microbiol* 62(5):1747–1751.
34. Casadaban MJ, Cohen SN (1980) Analysis of gene control signals by DNA fusion and cloning in *Escherichia coli*. *J Mol Biol* 138(2):179–207.
35. Meyer R, Figurski D, Helinski DR (1977) Physical and genetic studies with restriction endonucleases on the broad host-range plasmid RK2. *Mol Gen Genet* 152(3):129–135.
36. Elhai J, Wolk CP (1988) Conjugal transfer of DNA to cyanobacteria. *Methods Enzymol* 167:747–754.
37. Seib LO, Kehoe DM (2002) A turquoise mutant genetically separates expression of genes encoding phycoerythrin and its associated linker peptides. *J Bacteriol* 184(4):962–970.
38. Shen G, et al. (2006) Identification and characterization of a new class of bilin lyase: The *cpcT* gene encodes a bilin lyase responsible for attachment of phycocyanobilin to Cys-153 on the beta-subunit of phycocyanin in *Synechococcus* sp. PCC 7002. *J Biol Chem* 281(26):17768–17778.
39. Collier JL, Grossman AR (1992) Chlorosis induced by nutrient deprivation in *Synechococcus* sp. strain PCC 7942: Not all bleaching is the same. *J Bacteriol* 174(14):4718–4726.

Supporting Information

Shukla et al. 10.1073/pnas.1211777109

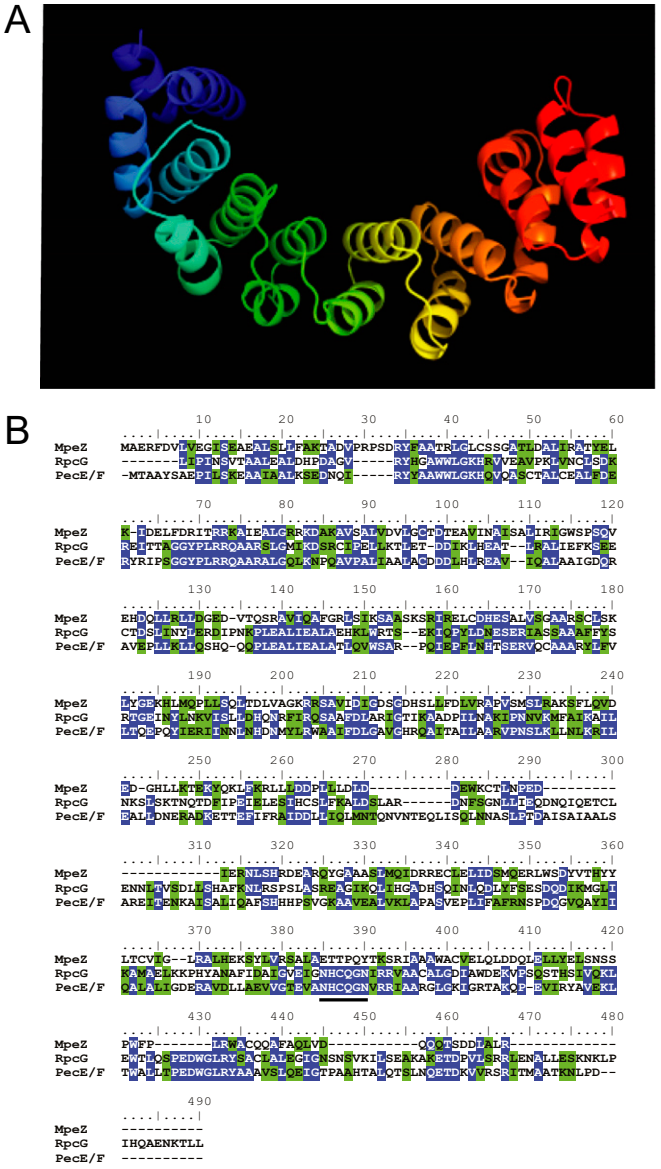

Fig. S1. MpeZ primary and secondary structural analyses. (*A*) Prediction of the secondary structure of MpeZ using Phyre2 (1). A total of 244 residues of 413 (59% of MpeZ sequence) were modeled with 99.9% confidence to the PBS lyase HEAT-like repeat family (2, 3) by the single highest scoring template. (*B*) ClustalW multiple sequence alignment (4) of deduced MpeZ (*Synechococcus* sp. RS9916), RpcG (*Synechococcus* sp. RS9916), and PecE/F fusion protein (*Mastigocladus laminosus*) using Bioedit stand-alone software with the default gap penalties. Characters highlighted in blue or green represent identical or similar residues, respectively. Black underlining demarks the sequence NHCQGN.

1. Kelley LA, Sternberg MJE (2009) Protein structure prediction on the Web: A case study using the Phyre server. *Nat Protoc* 4(3):363–371.
2. Fairchild CD, Glazer AN (1994) Oligomeric structure, enzyme kinetics, and substrate specificity of the phycocyanin alpha subunit phycocyanobilin lyase. *J Biol Chem* 269(12):8686–8694.
3. Andrade MA, Bork P (1995) HEAT repeats in the Huntington's disease protein. *Nat Genet* 11(2):115–116.
4. Thompson JD, Higgins DG, Gibson TJ (1994) CLUSTAL W: Improving the sensitivity of progressive multiple sequence alignment through sequence weighting, position-specific gap penalties and weight matrix choice. *Nucleic Acids Res* 22(22):4673–4680.

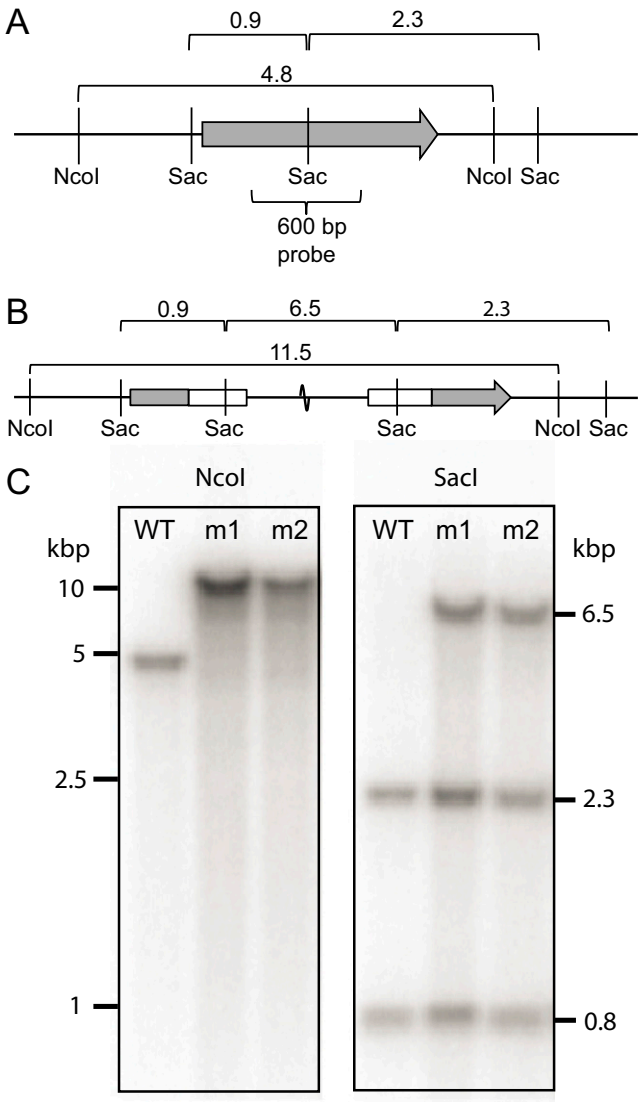

Fig. S2. Restriction maps and DNA blot analysis show *mpeZ* disruption in two representative *mpeZ* mutants. (*A*) Restriction map of wild-type (WT) 9916 at the *mpeZ* locus. (*B*) Restriction map of *mpeZ* mutant at the same locus. (*C*) DNA blot analysis of WT and two *mpeZ* insertion mutants using the 600-bp probe shown in *A*. Fifteen micrograms of genomic DNA from 9916 wild-type and putative *mpeZ* mutants were cut with NcoI and SacI for the analysis. Size markers are shown at the side of each blot.

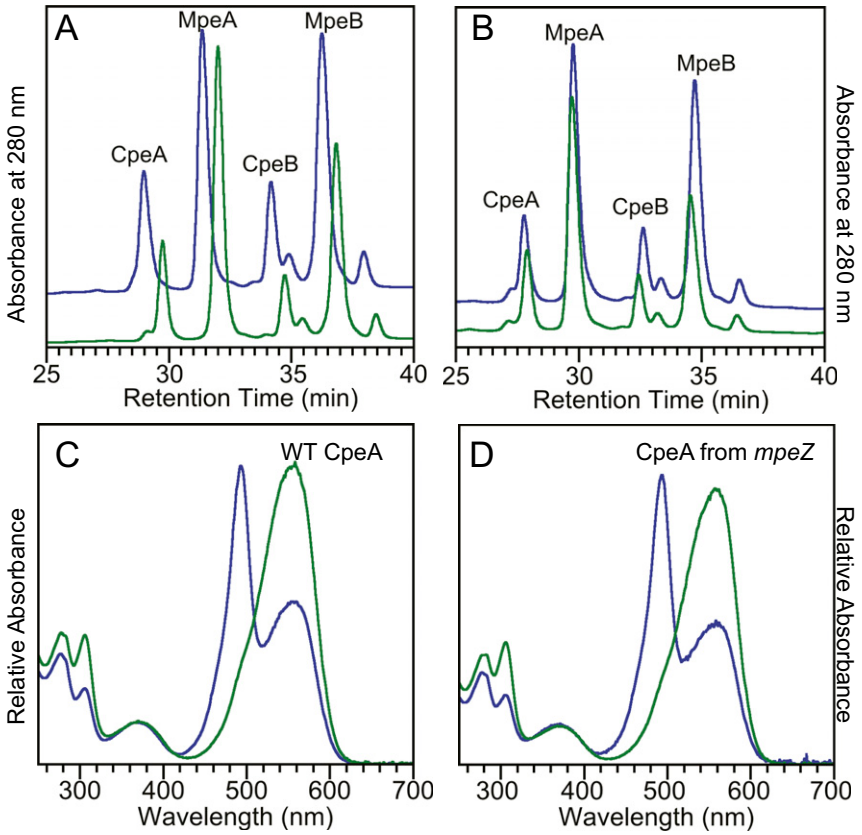

Fig. S3. HPLC separation and spectral analysis of PUB/PEB chromophorylation patterns for the phycobiliproteins MpeA, MpeB, CpeA, and CpeB. (*A*) The 280-nm chromatograms of wild-type (WT) 9916 phycobiliproteins isolated in blue light (BL) (blue line) and green light (GL) (green line) are shown, offset slightly to allow comparison of overlapping lines. The identity of each protein as determined by mass spectrometry is labeled above each peak. (*B*) The 280-nm chromatograms of the *mpeZ* mutant phycobiliproteins isolated in BL (blue line) and GL (green line) are shown offset. The identity of each protein as determined by mass spectrometry is labeled above each peak. (*C*) Spectra of CpeA from WT cells grown in BL (blue line) and GL (green line). (*D*) Spectra of CpeA from *mpeZ* mutant cells grown in BL (blue line) and GL (green line). HPLC was performed using a Waters Delta 600 controller and Waters 2996 photodiode array detector (Waters). Before HPLC, PBS samples were dialyzed against 5 mM Na phosphate buffer (pH 7.0), concentrated, and then combined (1:2, vol/vol) with 9 M urea (pH 2.0) for a final concentration of 6 M urea. This sample (~200 μL) was centrifuged before injecting on a C4 analytical column (250 × 4.6 mm: Hi-Pore RP304 column; Bio-Rad) that was previously equilibrated in 65% buffer A (0.1% trifluoroacetic acid (TFA; vol/vol in water) (buffer A), and 35% buffer B [2:1 acetonitrile: isopropanol containing 0.1% (vol/vol) TFA]. The flow rate for the column was 1.5 mL·min^{-1}. The linear gradient program used was as follows: 0–2 min, 65% buffer A, 35% buffer B; 2–37 min, 30% buffer A, 70% buffer B; 37–42 min, 100% buffer B; 42–47 min, 100% buffer B; 47–50 min, 65% buffer A, 35% buffer B; 50–55 min, 65% buffer A, 35% buffer B (all vol/vol). This method was modified from one described earlier (1). Phycobiliproteins were monitored from 200 to 700 nm.

1. Swanson RV, Glazer AN (1990) Separation of phycobiliprotein subunits by reverse-phase high-pressure liquid chromatography. *Anal Biochem* 188(2):295–299.

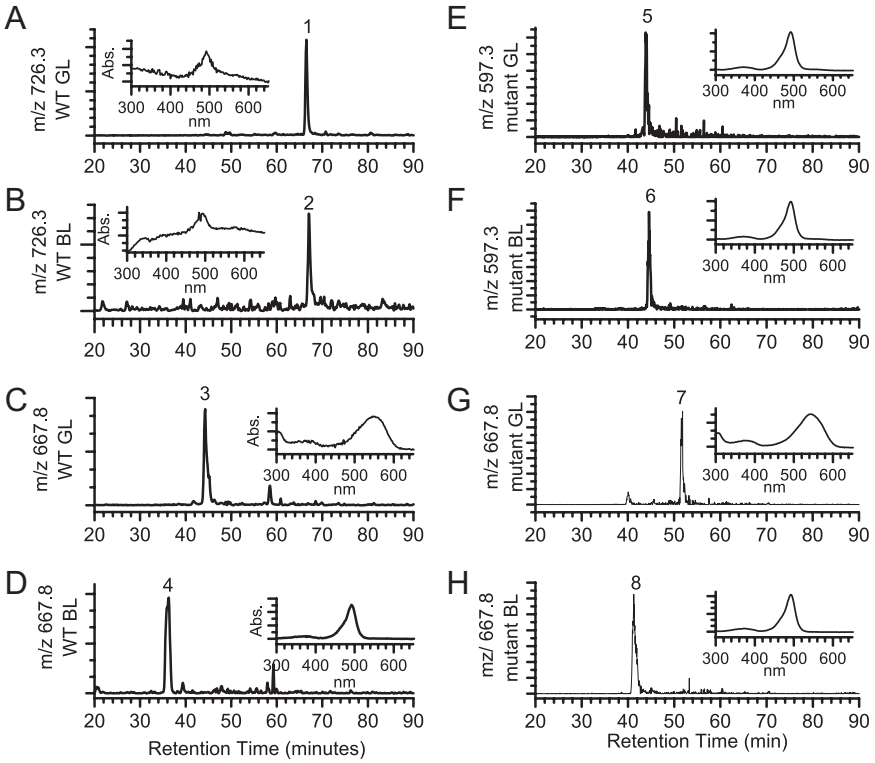

Fig. S4. Extracted ion chromatograms (EICs) and UV-visible (UV-VIS) absorption spectra (Abs.) for C75 and C140 of MpeA isolated from wild-type (WT) 9916 or *mpeZ* mutant cells grown under various conditions. (*A*) EIC for KC_{75}ATEGK $(M+2H)^{2+}$ at *m/z* 726.3 derived from WT cells grown in green light (GL). (*Inset*) The UV-VIS spectrum at retention time 66.5 min ("1" on the chromatogram) indicating that C75 is modified by PUB. (*B*) The EIC for KC_{75}ATEGK isolated from WT cells grown in blue light (BL). (*Inset*) UV-VIS spectrum at retention time 67.2 min ("2" on the chromatogram) indicating that PUB is the chromophore on C75. (C) EIC for $NDGC_{140}$SPR $(M+2H)^{2+}$ at *m/z* 667.8 derived from WT cells grown in GL. (*Inset*) UV-VIS spectrum at retention time 44.3 min ("3" on the chromatogram) suggesting that C140 is modified by PEB. (*D*) EIC for $NDGC_{140}$SPR $(M+2H)^{2+}$ at *m/z* 667.8 derived from WT cells grown in BL. The UV-VIS spectrum from retention time 36.0 min ("4" on the chromatogram) suggests that C140 is modified by PUB under these conditions. (*E*) EIC for C_{75}ATEGK $(M+2H)^{2+}$ at *m/z* 597.3 derived from *mpeZ* mutant cells grown in GL. (*Inset*) The UV-VIS spectrum at retention time 44.0 min ("5" on the chromatogram) indicating that C75 is modified by PUB. (*F*) EIC for C_{75}ATEGK $(M+2H)^{2+}$ at *m/z* 597.3 derived from *mpeZ* mutant cells grown in BL. (*Inset*) The UV-VIS spectrum at retention time 44.3 min ("6" on the chromatogram) indicating that C75 is modified by PUB. (*G*) EIC for $NDGC_{140}$SPR $(M+2H)^{2+}$ at *m/z* 667.8 derived from *mpeZ* mutant cells grown in GL. (*Inset*) The UV-VIS spectrum at retention time 51.5 min ("7" on the chromatogram) suggests that C140 is modified by PEB. (*H*) EIC for $NDGC_{140}$SPR $(M+2H)^{2+}$ at *m/z* 667.8 derived from *mpeZ* mutant cells grown in BL. The UV-VIS spectrum from retention time 41.0 min ("8" on the chromatogram) suggests that Cys_{140} is modified by PUB under these conditions. HPLC-separated and trypsin-digested phycobiliprotein samples from *mpeZ* mutant cells grown in GL were reconstituted in 40 μL of liquid chromatography/mass spectrometry (LC/MS) buffer A before analysis (BL samples were reconstituted in 10 μL). LC/MS buffer A was 97% (vol/vol) Omnisolve-grade water (EM Science), 3% (vol/vol) Omnisolve-grade acetonitrile (EM Science), and 0.1% (vol/vol) formic acid (LC/MS grade; Fluka). LC/MS buffer B was 97% (vol/vol) acetonitrile, 3% (vol/vol) water, and 0.1% (vol/vol) formic acid. The separation was performed with an Agilent 1200 capillary liquid chromatograph (Agilent Technologies) equipped with a diode array UV-VIS absorbance detector and a 500-nL flow cell. The column was 0.3 mm i.d., 150 mm long, and packed with 5 μm Zorbax SBC18-300 particles (Agilent). Three μl of each diluted sample were injected, and the peptides were separated at 4 μL/min with the following gradient: 5% buffer B for 15 min, ramp to 55% buffer B at 95 min, ramp to 85% buffer B at 100 min, hold at 85% buffer B for 10 min, re-equilibrate the column at 5% buffer B for 15 min (130 min total run time). The UV-VIS detector recorded absorption spectra from 250 to 750 nm at 2.5 Hz; chromatograms for 216, 490, 550, and 620 nm (to detect all peptides, PUB, PEB, and PCB modified peptides, respectively) were extracted by the computer as the diode array data were written to the hard drive. Tandem mass spectra were recorded in a data-dependent fashion with a Bruker HCT-Ultra PTM ion trap mass spectrometer (Bruker Daltonics) placed after the diode array detector. Intact peptide mass spectra were recorded from *m/z* 400–1800 in "standard enhanced" mode. The three most intense ions in each spectrum were selected for collisionally induced dissociation (CID) tandem MS. Singly charged ions were not fragmented, and each precursor ion could be selected only three times before being placed on an exclusion list for 1.20 min. Peptide ions were activated using "SmartFrag" mode, which ramped the activation energy from 0.4 to 2.0 V during the 40-ms fragmentation event; fragment mass spectra were recorded from *m/z* 200 to 1,800 in UltraScan mode. Samples isolated from wild-type cells were analyzed in a nearly identical fashion to the *mpeZ* mutant isolates except that a 150-min HPLC gradient was used. The presence of each specific biliprotein was confirmed by comparing the tandem mass spectra to the *Synechococcus* RS9916 peptide FASTA file downloaded from the J. Craig Venter Institute website (https://moore.jcvi.org/moore/SingleOrganism.do?speciesTag=RS9916&pageAttr=pageMain) using MASCOT 2.2 (Matrix Science Inc.) (1). The search parameters were a peptide mass error tolerance of ±1.2 Th ["Th" is an abbreviation for Thompson, the unit of mass/charge, and is equal to 1 u/e (1 atomic mass unit per fundamental charge on an electron)] and a fragment ion error tolerance of ±0.6 Th; +2 and +3 ions were preferred, and oxidation of methionine residues as well as modifications of cysteine by PEB/PUB (+586.27 Da) were considered. Bilin-containing peptides were confirmed manually using the following criteria: (*i*) the mass of the peptide had to match the predicted mass of a bilin-modified tryptic peptide, (*ii*) a large fragment ion corresponding to the neutral loss of the bilin upon CID (M-586) and/or the presence of a significant fragment ion at *m/z* 587 (intact bilin+H^+) had to be observed (2, 3, 4); and (*iii*) the UV-VIS absorption spectrum of the eluted peptide had to show an absorbance maximum at either 490 nm (for PUB) or 550 nm (for PEB).

1. Perkins DN, Pappin DJC, Creasy DM, Cottrell JS (1999) Probability-based protein identification by searching sequence databases using mass spectrometry data. *Electrophoresis* 20(18): 3551–3567.
2. Biswas A, et al. (2011) Characterization of the activities of the CpeY, CpeZ, and CpeS bilin lyases in phycoerythrin biosynthesis in *Fremyella diplosiphon* strain UTEX 481. *J Biol Chem* 286 (41):35509–35521.
3. Shen GZ, Leonard HS, Schluchter WM, Bryant DA (2008) CpcM posttranslationally methylates asparagine-71/72 of phycobiliprotein beta subunits in *Synechococcus* sp. strain PCC 7002 and *Synechocystis* sp. strain PCC 6803. *J Bacteriol* 190(14):4808–4817.
4. Bishop JE, et al. (1987) Chromopeptides from phycoerythrocyanin: Structure and linkage of the 3 bilin groups. *J Am Chem Soc* 109(3):875–881.

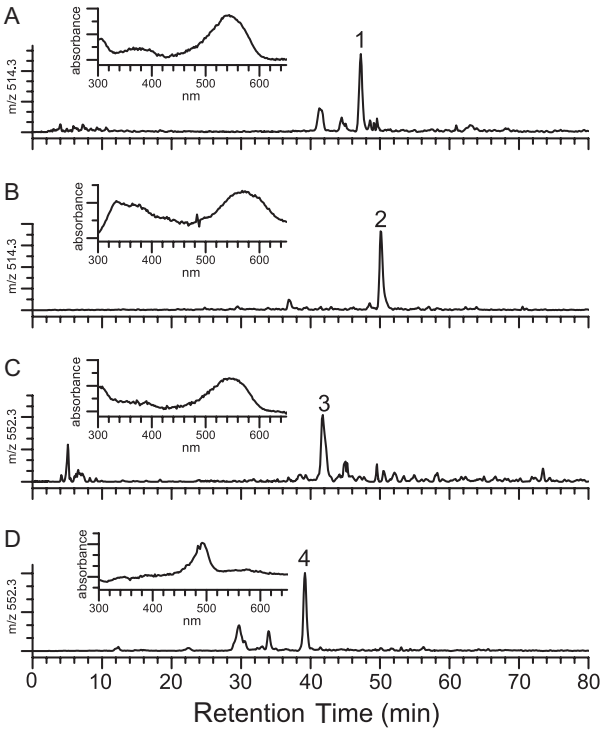

Fig. S5. Extracted ion chromatograms (EICs) and UV-visible (UV-VIS) spectra for tryptic peptides derived from CpeA isolated from wild-type 9916 cells grown in green light (GL) and blue light (BL). (*A*) EIC for C_{82}YR $(M+2H)^{2+}$ at *m/z* 514.3 derived from cells grown in GL. (*Inset*) The UV-VIS absorption spectrum at retention time 47.6 min ("1" on the chromatogram) indicating that C82 is modified by PEB. (*B*) EIC for C_{82}YR $(M+2H)^{2+}$ at *m/z* 514.3 derived from cells grown in BL. (*Inset*) The UV-VIS absorption spectrum at retention time 50.1 min ("2" on the chromatogram) indicating that C82 is modified by PEB. (*C*) EIC for AC_{139}APR $(M+2H)^{2+}$ at *m/z* 552.3 derived from cells grown in GL. (*Inset*) The UV-VIS absorption spectrum at retention time 42.0 min ("3" on the chromatogram) indicating that C139 is modified by PEB. (*D*) EIC for AC_{139}APR $(M+2H)^{2+}$ at *m/z* 552.3 derived from cells grown in BL. (*Inset*) The UV-VIS absorption spectrum at retention time 39.2 min ("4" on the chromatogram) indicating that C139 is modified by PUB.

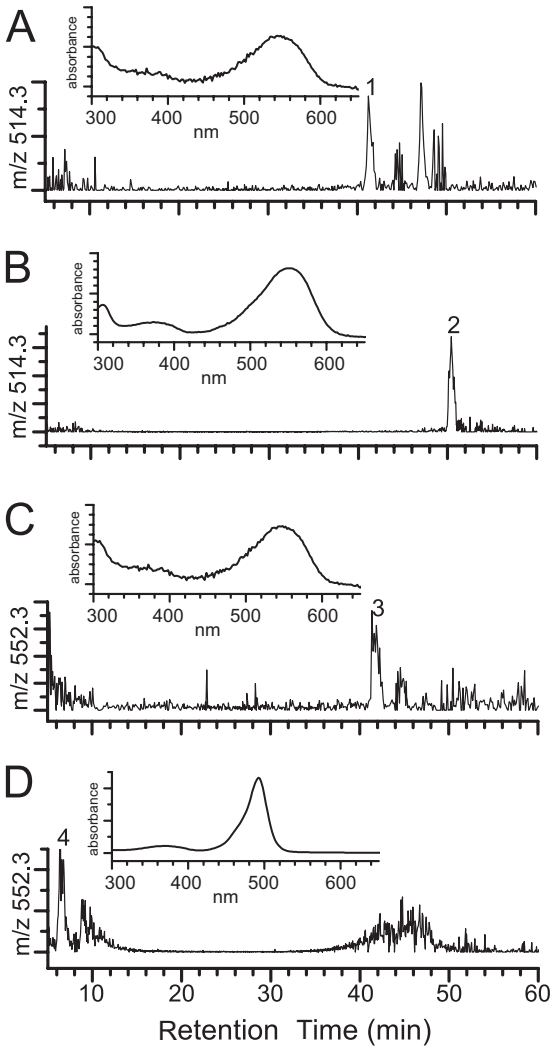

Fig. S6. Extracted ion chromatograms (EICs) and UV-visible (UV-VIS) spectra for tryptic peptides derived from CpeA isolated from *mpeZ* mutant cells grown in green light (GL) and blue light (BL). (*A*) EIC for C_{82}YR $(M+2H)^{2+}$ at *m/z* 514.3 derived from *mpeZ* mutant cells grown in GL. (*Inset*) The UV-VIS absorption spectrum at retention time 41.6 min ("1" on the chromatogram) indicating that C82 is modified by PEB. (*B*) EIC for C_{82}YR $(M+2H)^{2+}$ at *m/z* 514.3 derived from *mpeZ* mutant cells grown in BL. (*Inset*) The UV-VIS absorption spectrum at retention time 50.1 min ("2" on the chromatogram) indicating that C82 is modified by PEB. (*C*) EIC for AC_{139}APR $(M+2H)^{2+}$ at *m/z* 552.3 derived from *mpeZ* mutant cells grown in GL. (*Inset*) The UV-VIS absorption spectrum at retention time 41.5 min ("3" on the chromatogram) indicating that C139 is modified by PEB. (*D*) EIC for AC_{139}APR $(M+2H)^{2+}$ at *m/z* 552.3 derived from *mpeZ* mutant cells grown in BL. (*Inset*) The UV-VIS absorption spectrum at retention time 6.8 min ("4" on the chromatogram) indicating that C139 is modified by PUB.

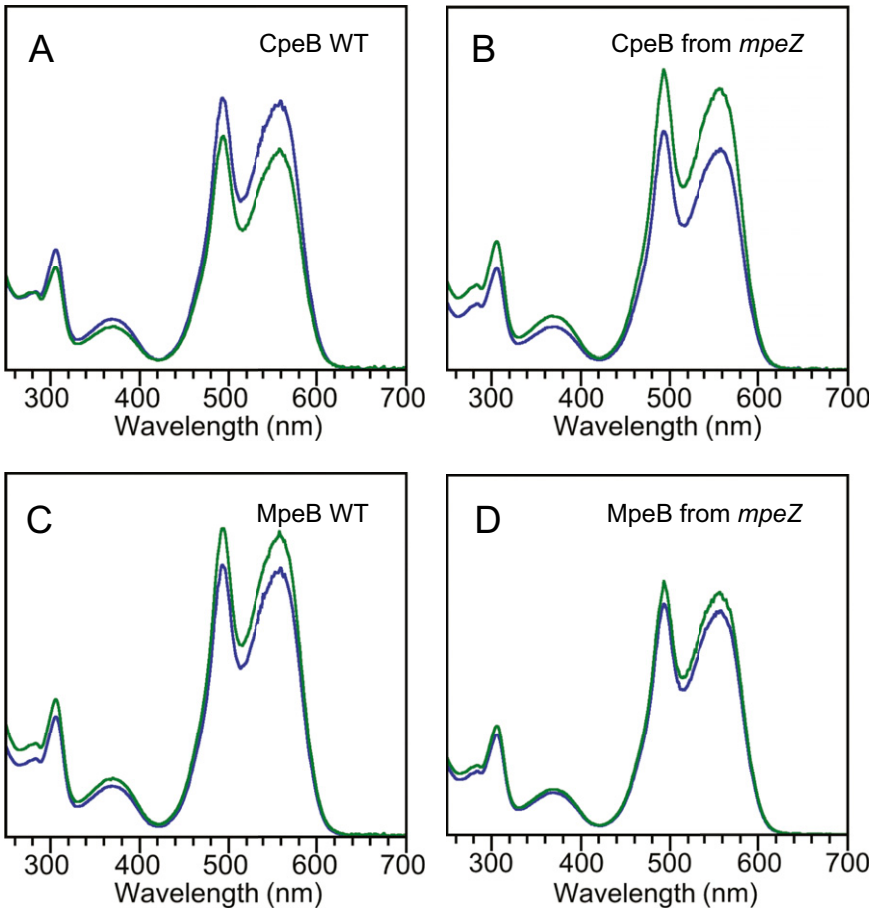

Fig. S7. Spectral analyses of the PUB/PEB chromophorylation patterns for CpeB and MpeB after HPLC. (*A*) Spectra of CpeB (from the chromatogram in Fig. S3*A*) from wild-type (WT) 9916 cells grown in blue light (BL) (blue line) and green light (GL) (green line). (*B*) Spectra of CpeB from *mpeZ* mutant cells (from the chromatogram in Fig. S3*B*). (*C*) Spectra of MpeB (from the chromatogram in Fig. S3*A*) from WT cells grown in BL (blue line) and GL (green line). (*D*) Spectra of MpeB from *mpeZ* mutant cells (from the chromatogram in Fig. S3*B*).

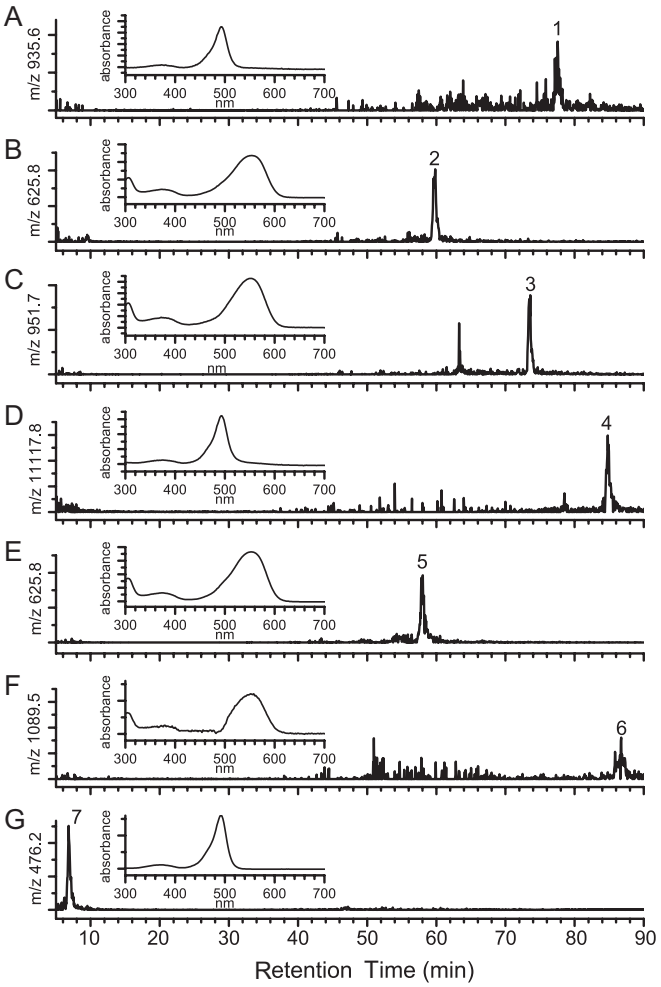

Fig. S8. Extracted ion chromatograms (EICs) and UV-visible (UV-VIS) absorption spectra for tryptic peptides of CpeB, MpeB, and RpcA isolated from a *mpeZ* mutant grown in green light (GL). (*A*) EIC for the peptide LDAVNAITSNASC$_{50}$IVSDAVTGM$^{Ox}{}_{59}$IC$_{61}$ENTGLIQAGGN$^{-Me}{}_{72}$C$_{73}$YPNR (M+5H)$^{5+}$ from CpeB at *m/z* 935.8. Cys$_{50}$ and Cys$_{61}$ are expected to be cross-linked by a bilin (1, 2); Met$_{59}$ is oxidized and Asn$_{72}$ is methylated (3); C73 is not modified. (*Inset*) The UV-VIS absorption spectrum at retention time 77.6 min ("1" on the chromatogram) indicating PUB as the chromophore. (*B*) EIC for the peptide MAAC$_{82}$LR (M+2H)$^{2+}$ from CpeB at *m/z* 625.8. (*Inset*) The UV-VIS absorption spectrum at retention time 59.4 min ("2" on the chromatogram) indicating that C82 is modified by PEB. (*C*) EIC for the peptide M$^{Ox}{}_{158}$ETTQGDC$_{165}$SALVAEAGSYFDR (M+3H)$^{3+}$ from CpeB at *m/z* 951.7 (Met158 is oxidized). (*Inset*) The UV-VIS absorption spectrum at retention time 73.5 min ("3" on the chromatogram) indicating that C165 is modified by PEB. (*D*) EIC for the peptide LDAVNAIAGNAAC$^{\dagger}{}_{50}$IVSDAVAGIC$_{60}$C$^{\dagger}{}_{61}$ENTGLTAPNGGVYTNR (M+4H)$^{4+}$ from MpeB at *m/z* 1117.8. Cysteines 50 and 61 are expected to be cross-linked by a bilin; cysteine 60 is not modified. (*Inset*) The UV-VIS spectrum at retention time 84.7 min ("4" on the chromatogram) indicating that the chromophore is PUB. (*E*) The EIC for peptide MAAC$_{82}$LR (M+2H)$^{2+}$ from MpeB at *m/z* 625.8. (*Inset*) The UV-VIS spectrum at retention time 59.0 min ("5" on the chromatogram) showing that C82 is modified by PEB. (*F*) EIC for the peptide AAVTQGDC$_{159}$ASLSAEAGSYFDM$^{Ox}{}_{172}$VISAIS (M+3H)$^{3+}$ from MpeB at *m/z* 1089.5; Met$_{172}$ is oxidized. (*Inset*) The UV-VIS absorption spectrum at 86.1 min ("6" on the chromatogram) showing that C159 is modified by PEB. (*G*) EIC for C$_{84}$SR (M+2H)$^{2+}$ from RpcA at *m/z* 476.2. (*Inset*) The UV-VIS spectrum at retention time 7.0 min ("7" on the chromatogram) indicating that PUB is the chromophore on C84.

1. Schoenleber RW, Leung SL, Lundell DJ, Glazer AN, Rapoport H (1983) Chromopeptides from phycoerythrins: Structure and linkage of a phycoerythrobilin tryptic tripeptide derived from a B-phycoerythrin. *J Am Chem Soc* 105(12):4072–4076.
2. Nagy JO, Bishop JE, Klotz AV, Glazer AN, Rapoport H (1985) Bilin attachment sites in the alpha-subunits, beta-subunits, and gamma-subunits of R-phycoerythrin: Structural studies on singly and doubly linked phycourobilins. *J Biol Chem* 260(8):4864–4868.
3. Shen GZ, Leonard HS, Schluchter WM, Bryant DA (2008) CpcM posttranslationally methylates asparagine-71/72 of phycobiliprotein beta subunits in *Synechococcus* sp. strain PCC 7002 and *Synechocystis* sp. strain PCC 6803. *J Bacteriol* 190(14):4808–4817.

Table S1. Plasmids used in this study

Plasmids	Relevant characteristics	Source
pColADuet-RS9916-mpeA	*mpeA* overexpression, N-terminal His tag	This study
pColADuet-RS9916-mpeB	*mpeB* overexpression, N-terminal His tag	This study
pColADuet-RS9916-cpeA	*cpeA* overexpression, N-terminal His tag	This study
pCDFDuet-RS9916-mpeZ	*mpeZ* overexpression	This study
PPebS	Phycoerythrobilin synthase overexpression	(1)
pCOLADuet-RS9916-mpeA-Cys83-Ala83	*mpeA* overexpression, Cys-83 mutated to Ala	This study
pCOLADuet-RS9916-mpeA-Cys140-Ala140	*mpeA* overexpression, Cys-140 mutated to Ala	This study
pCOLADuet-RS9916-mpeA-Cys75-Ala75	*mpeA* overexpression, Cys-75 mutated to Ala	This study
pCOLADuet-RS9916-mpeA-Cys83/140-Ala83/140	*mpeA* overexpression, Cys-83 and -140 mutated to Ala	This study
pCOLADuet-RS9916-mpeA-Cys75/140-Ala75/140	*mpeA* overexpression, Cys-75 and -140 mutated to Ala	This study
pCOLADuet-RS9916-mpeA-Cys75/83/140-Ala75/83/140	*mpeA* overexpression, Cys-75, -83, and -140 mutated to Ala	This study
pRL528	Helper plasmid, carries *mob*	(2)
pRK24	Conjugal plasmid, RK2 derivative	(3)
pMUT100	Suicide vector backbone used for homologous recombination	(4)
PASmpeZ	*mpeZ* gene interruption, carries a 1-kbp internal region of *mpeZ*	This study

1. Dammeyer T, Bagby SC, Sullivan MB, Chisholm SW, Frankenberg-Dinkel N (2008) Efficient phage-mediated pigment biosynthesis in oceanic cyanobacteria. *Curr Biol* 18(6):442–448.
2. Elhai J, Wolk CP (1988) Conjugal transfer of DNA to cyanobacteria. *Methods Enzymol* 167:747–754.
3. Meyer R, Figurski D, Helinski DR (1977) Physical and genetic studies with restriction endonucleases on the broad host-range plasmid RK2. *Mol Gen Genet* 152(3):129–135.
4. Brahamsha B (1996) A genetic manipulation system for oceanic cyanobacteria of the genus *Synechococcus*. *Appl Environ Microbiol* 62(5):1747–1751.

Table S2. Primers used in this study

Primer	Sequence (5′ to 3′)
9916mpeAfor	tctcccttatgcgactcctgcatt
9916mpeArev	tgcggccgtgtacaatacgattac
9916mpeBfor	tctcccttatgcgactcctgcatt
9916mpeBrev	tgcggccgtgtacaatacgattac
9916mpeZfor	cggccgcataatgcttaagtcgaa
9916mpeZrev	actcgacagccaggaagaagtgaa
CpeA-BamHI-for	acgggatccaagtctgtcgtgaccaccgttgtg
CpeA-HindIII-rev	gcgaagctttcccctgaagctatgagcctctaa
mpeA-Cys83/140-Ala-for1	aaggagatataccatgggcagcagccat
mpeA-Cys83-Ala-rev1	acgcttggccttctctttgccttcggtggc
mpeA-Cys83-Ala-for2	aaagagaaggccaagcgtgacttcgttcac
mpeA-Cys140-Ala-rev1	tcatgtcgcgaggggaggcaccgtcgtta
mpeA-Cys140-Ala-for2	atgcgtaacgacggtgcctcccctcgcgaca
mpeA-Cys140-Ala-for2	taccagactcgagggtaccgacgt
mpeA-Cys75-Ala-for2	agcctcgtaaggccgccaccgaaggcaaa
mpeA-Cys75-Ala-rev1	tttgccttcggtggcggccttacgaggct
mpeZ-out-for1	aaggtcccagaggccatggccgcctt
mpeZ-transrev1	aagggcatcggtcgacgctctccctt
mpeZ-transfor2	ttattgaagcatttatcagggttatt
mpeZ-out-rev2	ttgttagctttaggtttggatagcgtt
mpeZ-probe-for	agcctcatcacgatggctcagatt
mpeZ-probe-rev	aagatgccaaggctgtttctgctc
pMUT100-test-for	tcctgctcgcttcgctacttggagcca
pMUT100-test-rev	actcctgcattaggaagcagcccagt